Carbohydrate Polymers 212 (2019) 142–149

Contents lists available at ScienceDirect

Carbohydrate Polymers

journal homepage: www.elsevier.com/locate/carbpol

Mentha piperita essential oils loaded in a chitosan nanogel with inhibitory effect on biofilm formation against *S. mutans* on the dental surface

Behnam Ashrafi[a], Marzieh Rashidipour[a], Abdolrazagh Marzban[a], Setareh Soroush[a,b], Mojgan Azadpour[a], Somayeh Delfani[a,b,*], Parvin Ramak[c]

[a] Razi Herbal Medicines Research Center, Lorestan University of Medical Sciences, Khorramabad, Iran
[b] Department of Microbiology, School of Medicine, Lorestan University of Medical Sciences, Khorramabad, Iran
[c] Research Division of Natural Resources, Lorestan Agricultural and Natural Resources Research and Education Center, AREEO, Khorramabad, Iran

ARTICLE INFO

Keywords:
Mentha piperita
Antibiofilm activity
Streptococcus mutans
Chitosan nanogel
Dental caries

ABSTRACT

Mentha piperita essential oils (MPEO) were loaded into chitosan nanogel to use as antibiofilm agent against *Streptococcus mutans* and to protect its dental plaque. Chitosan nanoparticles (CsNPs) were prepared by sol-gel method using linking bridge of tripolyphosphate (TPP). Physiological properties of MPEO-CNs were assessed by FTIR, SEM/EDX, DLS and zeta potential. Release kinetics, MIC and MBC were determined for MPEO-CNs. Expression of biofilm-associated genes including 8 genes: *grf*B, C and D, *brp*A, *spa*P, *gbp*B, *rel*A and *vic*R was investigated at the presence of sub-MIC of MPEO-CNs. Most abundant bioactive compounds of MPEO were l-menthol (45.05%) and l-menthal (17.53%). SEM/EDX exhibited successful entrapment of MPEO into CsNPs followed by the changes in abundance of elemental peaks. A signal at 1737 cm^{-1} on chitosan spectrum was attributed to the carboxylic (C═O) groups overlapped by MPEO incorporation. A new signal at 2361 cm^{-1} was assigned to electrostatic interactions of amine groups in chitosan with phosphoric units of TPP within the MPEO-chitosan. MPEO incorporation into porous nanogel decreased monodispersity of the nanoparticles and then raises z-average. Maximum release of MPEO was about 50% during 360 h in a hydroalcoholic solvent at ambient temperature. The adherence of bacterial cells showed high sensitivity to the nanoformulation of MPEO compared with unloaded chitosan-nanogel. Antibiofilm inhibition of *S. mutans* occurred in 50 and 400 µg/mL for MPEO-CNs and unloaded-nanogel, respectively. Among biofilm synthesis genes, *gtf*B, *gtf*C, *gtf*D were slightly affected by MPEO-CNs treatment, while *gbp*B, *spa*P, *brp*A, *rel*A, and *vic*R genes underwent significant down-regulation in the presence of both unloaded-nanogel and MPEO-loaded-nanogel. This study demonstrated that the MPEO-CNs promised an efficient nanoformulation with the greatest inhibitory action against some glycosyltransferase genes (*gtf*B, C and D) as important enzymes involved in extracellular polymers. Finally, the results concluded that MPEO-CNs have a potential use as antibiofilm agent in toothpaste or mouth washing formulations.

1. Introduction

Currently, biopolymer systems have been developed as efficient materials due to their inherent potential such as eco-friendly, biodegradability, biocompatibility, low toxicity and low immunogenicity, etc (El-Feky, Sharaf, El Shafei, & Hegazy, 2017). Chitosan is prepared from deacetylation of chitin with different molecular weights. One of the most important features is that chitosan possesses an excellent capacity for loading of drugs and bioactive compounds as nanosystem formulations (Kumari, Yadav, & Yadav, 2010). Hydrogel based-CsNPs called nanogel forms nanostructural networks that can entrap drugs and bioactive compounds (Oh, Lee, & Park, 2009). Because the natural chitosan molecules are cationic polymers, most compounds with negative charge can actively bind to their positive groups without chemical reactions or harsh modifications (Nagpal, Singh, & Mishra, 2010). Depending on the interactions involved in drug-nanogel incorporation, the release of drug can be controlled as a sustained release delivery system (Wu, Shen, Banerjee, & Zhou, 2010). CsNPs have been immensely applied for encapsulating bioactive molecules including anticancer drugs, antimicrobial compounds, vaccines, genes, plant-derived molecules and, etc (Cheung, Ng, Wong, & Chan, 2015; Nagpal et al., 2010; Rao, Reddy, Lee, & Kim, 2012). CsNPs are among the most-

* Corresponding author at: Razi Herbal Medicines Research Center, Lorestan University of Medical Sciences, Khorramabad, Iran.
E-mail addresses: behnamashrafi67@gmail.com (B. Ashrafi), m_rashidi80@yahoo.com (M. Rashidipour), marzban86@gmail.com (A. Marzban), soroush_setareh@yahoo.com (S. Soroush), mojganazadpour@yahoo.com (M. Azadpour), somayehdelfani@gmail.com (S. Delfani).

https://doi.org/10.1016/j.carbpol.2019.02.018
Received 7 October 2018; Received in revised form 17 December 2018; Accepted 6 February 2019
Available online 07 February 2019
0144-8617/

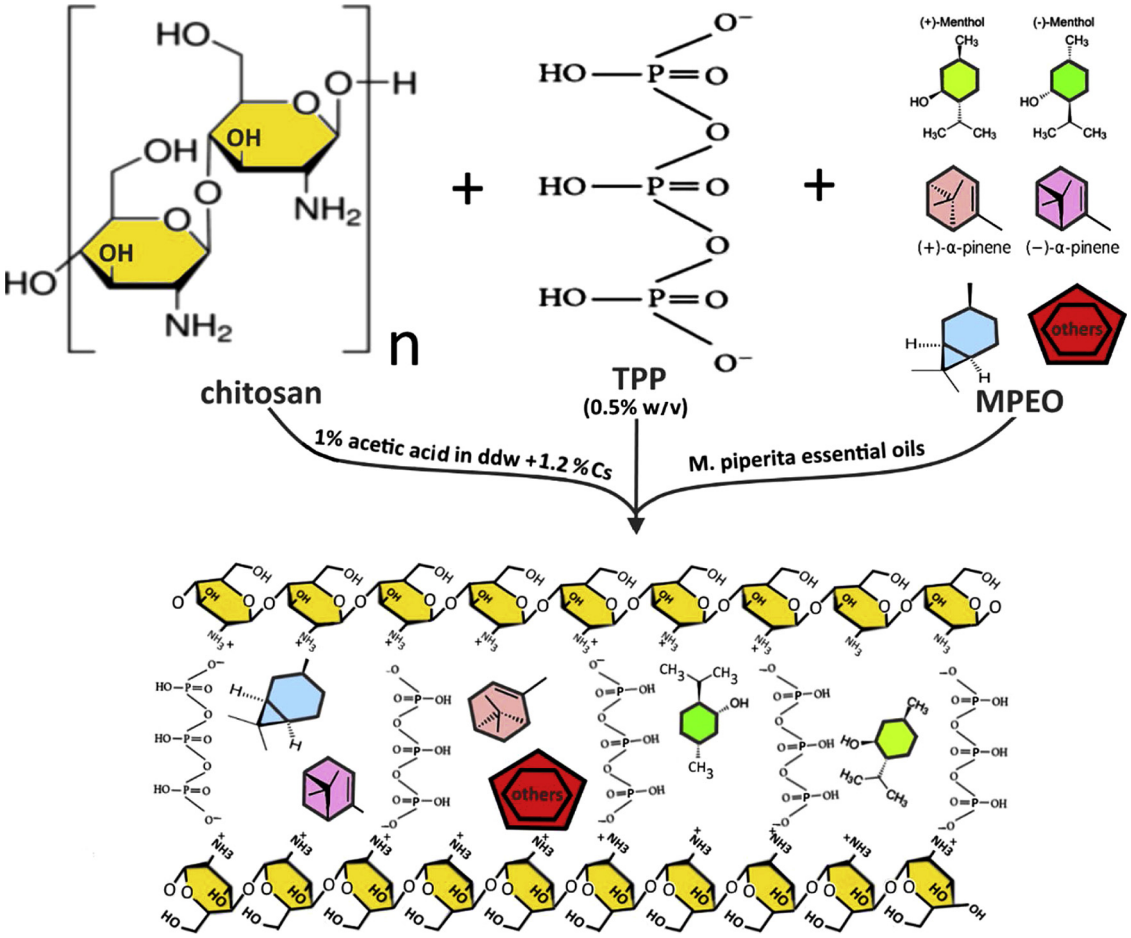

Fig. 1. Schematic illustration of chitosan nanogel synthesis and loading MPEO as a one-step phase fabrication.

widely used polysaccharides in the development of drug carriers due to their various advantages for drug delivery, especially for volatile compounds (Mohammadi, Hashemi, & Hosseini, 2015). Moreover, these nanoporous systems protect drugs against adverse interactions such as enzyme inactivation and hydrolyzing reactions (Barzegar, Ghaderi Ghahfarokhi, Sahari, & Azizi, 2016; Woranuch & Yoksan, 2013). Plant-derived bioactive extracts were commonly encapsulated into CsNPs by various methods such as ionic gelation, microemulsion, organic solvent evaporation and precipitation. These encapsulation methods improve drug stability with controlled release at the site of drug effect (Bernkop-Schnürch & Dünnhaupt, 2012; Beyki et al., 2014).

Dental caries is defined as a mineral alteration of the dental tissue and many causes may be responsible for this occurrence (Oong, Griffin, Kohn, Gooch, & Caufield, 2008). Amongst some biological factors, microbial biofilm has a critical role in the progression of dental decay (Marsh, 2010). Generally, the biofilm is a complicated matrix containing proteins and exopolysaccharides providing a physiological barrier for bacterial cells and protecting them against antimicrobial agents (Arshia Khan, Khan, Ahmed, Taha, & Perveen, 2017; Ikram et al., 2016). *S. mutans* is of the most famous biofilm forming bacterium inhabiting the mouth cavity and is associated with dental plaque. This species exerts a mineralizing effect on the dental structure by acidifying mouth environment through the production of organic acids from food residues (Koo, Xiao, Klein, & Jeon, 2010). To inhibit the formation of biofilm and protect against bacterial dental mineralization, many antimicrobial agents are available. Nevertheless, these agents produce side effects such as fluorosis, chromatism, dysgeusia, burning sensation, ulcerative lesions, and enamel erosion. Since dental caries is being magnified as a serious concern for global public health, therapeutic alternatives to improve oral health seem to be of essential importance (Seneviratne, Zhang, & Samaranayake, 2011).

Numerous plant essential oils are found to act as antibiofilm agents against mouth-inhabiting bacteria, especially *S. mutans* (Kim et al., 2015). *Mentha piperita* essential oils have been reported to possess several biological actions, such as antibacterial, antifungal, antiviral and larvicidal activities (Sandasi, Leonard, Van Vuuren, & Viljoen, 2011). Moreover, studies have shown that MPEO is nontoxic for human while it could strongly kill some pathogens with a Lethal Dose (LD_{50}) of 2000 mg/kg (Beyki et al., 2014). Considering the high exceptional potential of MPEO, this study focused on the formulation of MPEO encapsulated into CsNPs to be used as antibiofilm agent against the growth and biofilm formation of *S. mutans*.

2. Materials and methods

2.1. Compositional analysis of MPEO

The GC–MS was carried out on Agilent 6890 N GC coupled with Agilent 5973 mass selective detector (MSD) operating in Electron Ionization (EI) mode at 70e, fitted with an HP-5 column (30 m × 0.25 mm, i.d., 0.25 μm film thickness) and SPB-1 column (30m × 0.25 mm, i.d., 0.25 μm film thickness). The temperature of the column was adjusted from 40 to 230 °C with scanning time of 2 °C/min and then constantly maintained at 230 °C for 30 min. The injector and interface temperatures were programmed at 250 °C. Helium was selected as the carrier gas that was adjusted to a flow rate of 0.9 mL/min. Identification of chemical components was performed by comparing MS spectra with known compounds in Wiley 7 n/NIST05 mass spectra

Table 1
Characteristics of primers used in the study of the genes associated with biofilm formation.

Gene	Gene description	Primer sequences (5 -3)	
gtf B	Glucosyltransferase-I	Forward:	AGCAATGCAGCCAATCTACAAAT
		Reverse:	ACGAACTTTGCCGTTATTGTCA
gtf C	Glucosyltransferase-SI	Forward:	GGTTTAACGTCAAAATTAGCTGTATTAGC
		Reverse:	CTCAACCAACCGCCACTGTT
gtf D	Glucosyltransferase-S	Forward:	ACAGCAGACAGCAGCCAAGA
		Reverse:	ACTGGGTTTGCTGCGTTTG
*brp*A	Biofilm regulatory protein A	Forward:	GGAGGAGCTGCATCAGGATTC
		Reverse:	AACTCCAGCACATCCAGCAAG
*spa*P	Cell surface antigen *Spa*P	Forward:	GACTTTGGTAATGGTTATGCATCAA
		Reverse:	TTTGTATCAGCCGGATCAAGTG
*gbp*B	Secreted antigen *Gbp*B/*Sag*A	Forward:	ATGGCGGTTATGGACACGTT
		Reverse:	TTTGGCCACCTTGAACACCT
*rel*A	GTP pyrophosphokinase	Forward:	ACAAAAAGGGTATCGTCCGTACAT
		Reverse:	AATCACGCTTGGTATTGCTAATTG
*vic*R	Response regulator	Forward:	TGACACGATTACAGCCTTTGATG
		Reverse:	CGTCTAGTTCTGGTAACATTAAGTCCAATA
16SrRNA	16S rRNA	Forward:	CCTACGGGAGGCAGCAGTAG
		Reverse:	CAACAGAGCTTTACGATCCGAAA

Table 2
Chemical compositions of *M. piperita* essential oils identified by GC–MS analysis.

Retention time	Compound	Area	%
5.171	2-Hexenal	5823496	0.15
7.286	*α*-Pinene	31561202	0.80
7.645	Camphene	892791	0.02
8.531	Sabinene	16254263	0.41
8.749	*β*-Pinene	37583490	0.95
9.315	Myrcene	6985234	0.18
9.56	3-Octanol	5379862	0.14
9.812	l-Phellandrene	2446353	0.06
10.383	*α*-Terpinene	12563440	0.32
10.578	*p*-Cymene	4001752	0.10
10.692	dl-Limonene	86355551	2.18
10.978	1,8-Cineole	168969523	4.26
11.601	*Δ*-3 Carene	7100536	0.18
12.047	ϒ-Terpinene	17852373	0.45
12.595	trans-Sabinene hydrate	23456801	0.59
13.264	Terpinolen	5349578	0.13
14.15	Iso amyl iso valerate	5871517	0.15
14.464	Thujone	512473	0.01
16.785	L-menthal one	624528299	17.53
17.036	Menthofuran	339852051	8.58
17.179	neo-Menthol	171456452	4.33
18.242	l-Menthol	1785269476	45.05
20.025	Pulegone	29144217	0.74
20.94	Piperitone	24125946	0.61
21.694	3-menthene	16475240	0.42
22.883	cis-Carane	325874547	8.22
23.231	Neoisomenthyl acetate	18547094	0.47
23.157	trans-Carane	7201213	0.18
26.278	*β*-bourbonene	8365895	0.21
26.586	*β*- elemene	2288245	0.06
27.615	trans-Caryophyllene	30748524	0.78
28.524	trans-*β*-Farnesene	6837489	0.17
29.073	Germacrene-D	31743358	0.80
29.33	bicyclogermacrene	5895892	0.15
29.775	*δ*-Cadinene	1178533	0.03
30.701	Caryophyllene oxide	1984338	0.05
30.861	Viridiflorol	9258741	0.23
32.736	Eicosane	12587425	0.32
33.456	Di-isobutyl phthalate	654258	0.02

libraries and NIST GC retention data webbook (http://webbook.nist.gov/chemistry/)database

2.2. MPEO extraction and chitosan-based encapsulation

The MPEO was extracted by hydrodistillation method in a Clevenger apparatus. MPEO-CsNPs were prepared according to a method described by Keawchaoon and Yoksan (2011). Briefly, 40 mL of chitosan solution (1.2% w/v) was prepared in distilled water containing 1% of acetic acid. After 24 h, 0.3 *g* Tween 60 was added to the mixture and homogenized by stirring at 60 °C for 2 h. The MPEO was added dropwise into the stirring mixture and agitated for 20 min A set of experiments including 1:0, 1:0.25, 1:0.50, 1:0.75, 1:1.00 and 1:1.25 chitosan to MPEO were performed to obtain an efficient formulation. A 40 mL of TPP solution (0.5% w/v) was dropped into an o/w emulsion and was stirred for 30 min. The solution mixture was centrifuged at 10,000 rpm for 10 min at 25 °C, synthesized nanogel was washed with Tween 60 solution (1% v/v) and distilled water to remove free MPEO. Finally, nanogel was dispersed in distilled water and kept at 4 °C for further study. Summary of the chitosan nanogel synthesis containing MPEO has been presented in the Fig. 1.

2.3. Analysis of MPEO- CsNPs formation

Formation of MPEO-CsNPs was studied using analytical and instrumental methods. Chitosan nanostructure and corresponding MPEO-CsNPs were taken for SEM/EDX analyses. FTIR spectra were conducted using a Fourier transform infrared spectrometer at a resolution of 4 cm^{-1} from 4000 to 400 cm^{-1}. Zeta potential and particle diameter were measured at 20 °C using a Malvern model 3600 Zetasizer (UK) equipped with a He–Ne laser operating at 4.0 mW and 633 nm with a fixed scattering angle of 90° (Keawchaoon & Yoksan, 2011).

2.4. Release kinetics study of MPEO-CsNPs

A 20 mg of MPEO-CsNPs was dispersed in phosphate buffer saline and stirred at ambient temperature. The samples were collected at regular times and centrifuged at 9000 rpm at 25 °C for 5 min. The amount of MPEO released into the supernatant was measured using spectrophotometer at 275 nm. Finally, the cumulative percent of the released amount was calculated using the following formula (Keawchaoon & Yoksan, 2011):

$$\text{Cumulative release}(\%) = \sum_{t=0}^{t} \frac{Mt}{M0} \times 100$$

2.5. Biofilm susceptibility

The effect of MPEO-CsNPs on *S. mutans* biofilm formation was examined by the microdilution method. The results were defined as minimum biofilm inhibition concentration (MBIC). Briefly, a two-fold

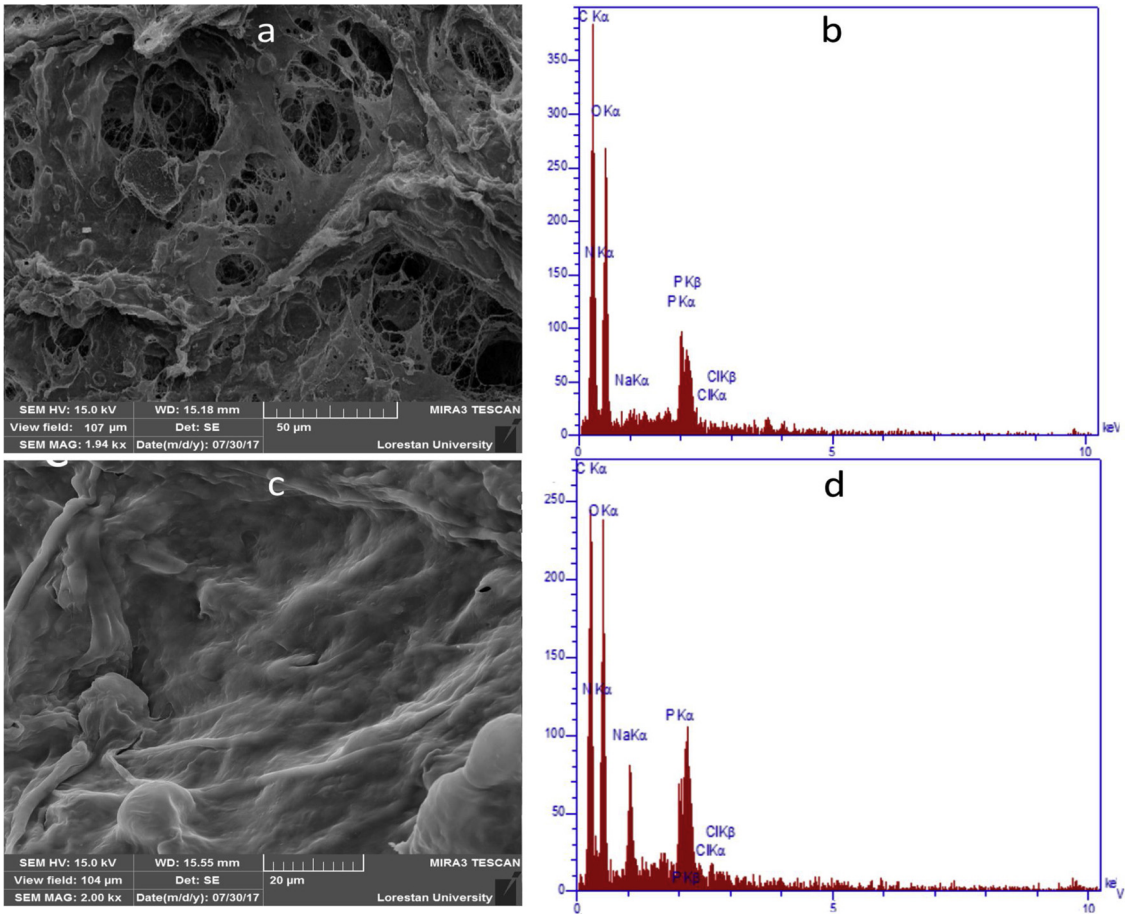

Fig. 2. Scanning electron microscopy (SEM) micrographs at 15 kV of unloaded chitosan nanogel and MPEO- chitosan nanogel (a and c) and their corresponding EDX microanalysis spectra (b and d).

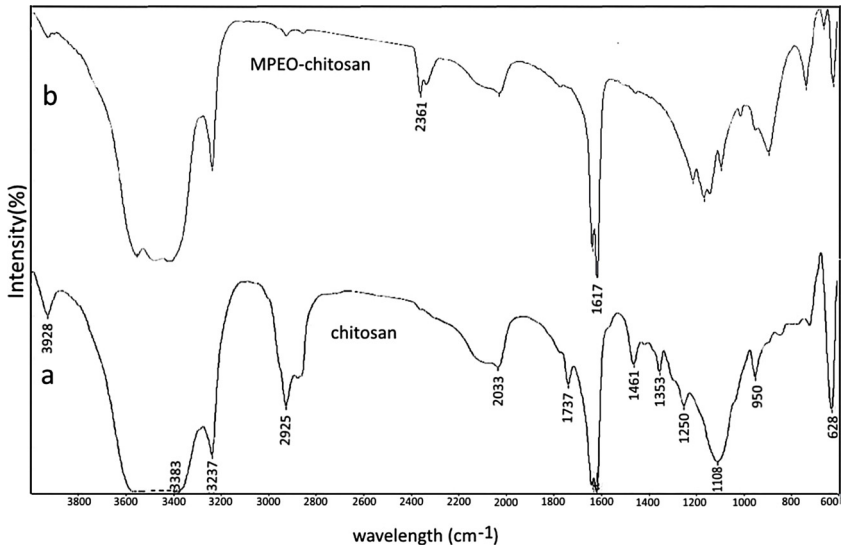

Fig. 3. Fourier transform infrared spectroscopy (FTIR) spectra unloaded-chitosan nanogel and MPEO-chitosan nanogel.

serial dilution of samples was prepared in 96-well polystyrene plates containing TPY broth (200 mL/well). MPEO-CsNPs were tested at the range of 400 to 50 µg/mL. A 20 mL of bacterial cell suspensions were inoculated into each plate well (5×10^7 cfu/mL). Bacterial growth was monitored in an anaerobic incubator (20% CO_2, 80% N_2, 37 °C, 24 h) and cell absorbance was measured at 595 nm. Firstly, free cells in the supernatants from each well were removed by washing with PBS at pH 7.2. The biofilm was fixed with ethanol (15 min), air dried at room temperature, stained (5 min) with 0.1% (w/v) Crystal Violet (Sigma) and rinsed thoroughly with water until control wells appeared colorless. Biofilm formation was quantified by the addition of 200 mL of 95% ethanol to each Crystal Violet-stained well. The minimum biofilm inhibition concentration (MBIC) was defined as the lowest concentration of the agent that showed 50% or more inhibition on the formation of

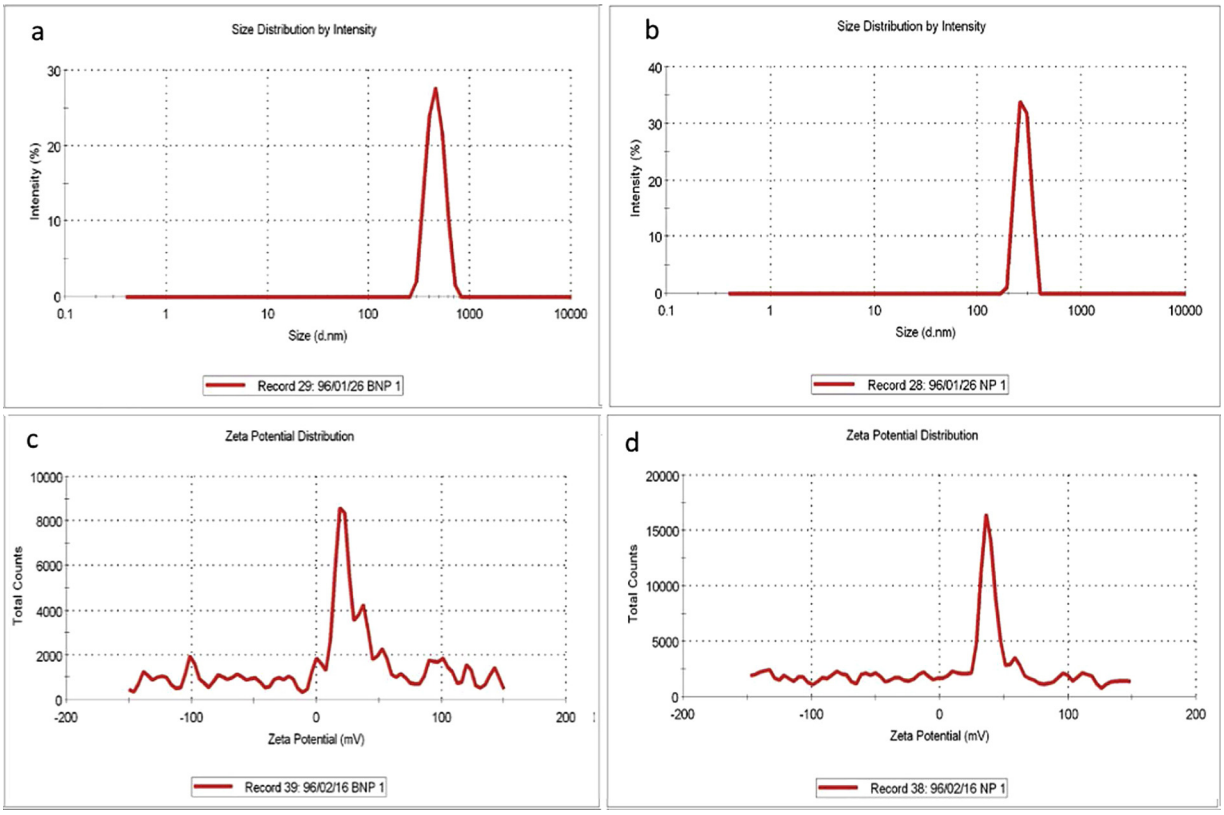

Fig. 4. Particle size distributions of unloaded-chitosan nanogel (a) and MPEO- chitosan nanogel (b). Zeta potential distribution within the surface of unloaded-chitosan nanogel (c) and MPEO- chitosan nanogel (d).

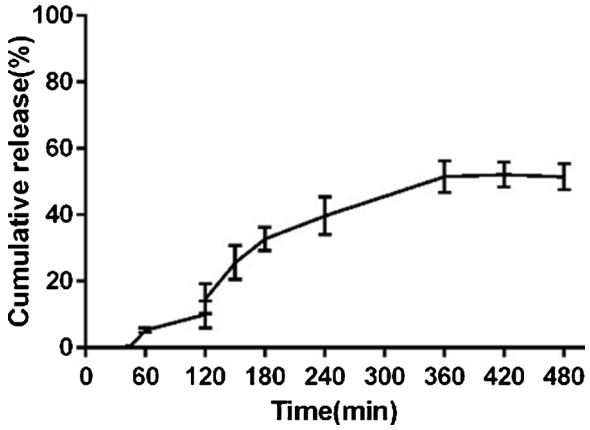

Fig. 5. Kinetic release of MPEO from chitosan nanogel in PBS. Cumulative release of MPEO in 480-h time course was calculated as a percentage of total MPEO loaded into chitosan nanogel.

biofilm (Ebrahimipour, Moradi, Mehrdad, Marzban, & Alaee, 2011; Xiao et al., 2007).

2.6. Bacterial adherence

The effect of MPEO-CsNPs on bacterial adherence was determined using Single-channel direct-rooted teeth. The teeth were directly washed with normal saline solution, 3 mL of 25.5% sodium hypochlorite and then 3 mL 17% EDTA to remove the smear layer. After the washing step, the teeth were autoclaved at 121 °C for 15 min. Briefly, the teeth were immersed in bacterial suspension (1×10^7 CFU/mL) with various concentrations of MPEO-CsNPs and incubated under the influence of CO_2 at 37 °C for 48 h in anaerobic conditions. Adherence activity was induced by agitation of bacterial culture in a shaker incubator at 100 rpm at 37 °C for 90 min. Subsequently, the samples were washed with PBS to remove non-adherent bacteria and transferred to a new tube. Finally, the biofilm formed at the surface was measured by staining with 0.1% safranin (Kim et al., 2015).

2.7. Real-time polymerase chain reaction (PCR) analysis

A real-time PCR was performed to evaluate the effect of the MPEO-CsNPs on gene expression of *S. mutans*. The subminimum inhibitory effective concentration of the MPEO-CsNPs was treated. After 24 h of culture, total RNA was isolated from *S. mutans* using a total RNA purification Kit, and cDNA was synthesized. The amplification was performed using a StepOnePlus Real-Time PCR system with QPCR SYBR Green Mixes. 16SrRNA was used as an internal control (Kim et al., 2015). Eight pairs of primers associated with biofilm formation were used in this study. These primers were designed by Kim et al. (2015), which are listed in Table 1

2.8. Statistical analysis

Statistical analyses of the results of mutagenicity testing for the different parameters; mutagenic index (MI), the mutagenic potential (M), induction factor (I) and analysis of variance (ANOVA) were carried out according to Anjum and Malik (2013).

3. Results and discussion

3.1. GC–MS analysis of MPEO chemical compositions

The chemical composition of MPEO was identified using GC–MS analysis. Forty compounds were identified in the MPEO in which predominant compounds were l-Menthol with 45.05% and then l-menthal

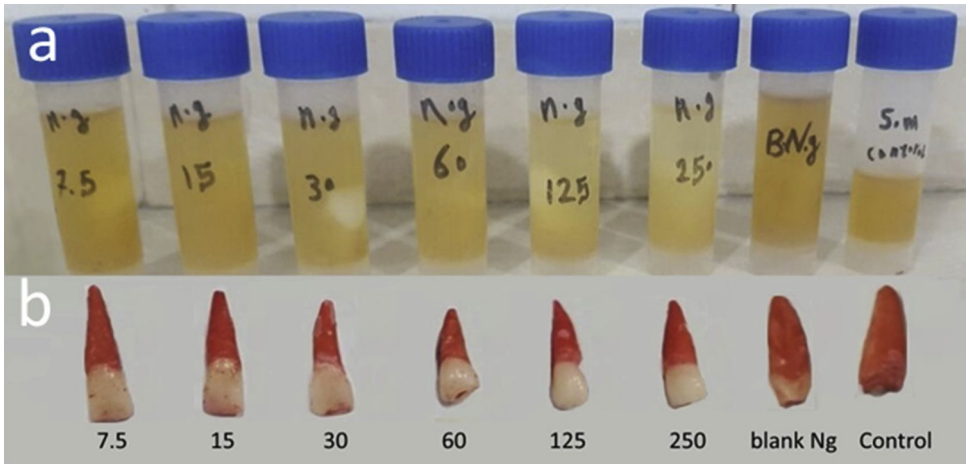

Fig. 6. Antibiofilm activity of MPEO-CsNPs against *S. mutans.* Growth of the bacterium in the presence of different concentrations of MPEO-CsNPs (a) and the effect of MPEO-CsNPs on biofilm formation by the bacterium on the dental surface.

Table 3
Antibiofilm inhibition of *S. mutans* in the three concentrations presented as MBIC (μg/mL).

treatment	MPEO-CNs (μg/mL)				unloaded-nanogel(μg/mL)			
MBIC (μg/mL)	NG400	NG200	NG100	NG50	BNG400	BNG200	BNG100	BNG50
Cell Inhibition (%)	0.72 ± 0.05	0.66 ± 0.06	0.65 ± 0.10	0.57 ± 0.17	0.47 ± 0.01	0.43 ± 0.02	0.43 ± 0.014	0.35 ± 0.1

with 17.53%. Those compounds that quantified up to 1% were identified as menthofuran (8.58%), cis-carane (8.22%), neo-menthol (4.33%), 1,8-cineole (4.36%) and dl-limonene (2.18%). The others were minor components as seen in Table 2. Several studies have confirmed the antibacterial activity of MPEO against gram-positive and gram-negative bacteria. Singh, Shushni, and Belkheir (2015) reported that an aqueous extract of *M. piperita* showed great inhibition against *S. aureus*, *S. pyogenes*, and *K. pneumonia*. Therefore, it is found to have a wide spectrum of antibacterial activity of different extracts of *M. piperita* against gram-positive and gram-negative bacteria as well as fungal species such as *Alternaria alternaria*, *Fusarium tabacinum*, *Fusarium oxyporum*, and *Aspergillus fumigates* (Moghtader, 2013). Due to large amounts of existing menthol derivatives in *M. piperita,* the various biological activities could be attributed to these compounds (Saharkhiz et al., 2012).

3.2. Characterization of MPEO-CsNPs

Morphological properties of MPEO-CsNPs were studied by SEM micrograph analysis. Fig. 2 presents SEM micrograph taken from CsNPs without MPEO loading and those nanogel formulation loaded with MPEO. As seen in this micrograph, MPEO mixture was entrapped by the porous structure of chitosan nanopolymer. EDX microanalysis of chitosan nanostructure and related MPEO-CsNPs exhibited changes in abundance of elemental peaks. As seen in Fig. 2b and d, carbon (CKα), sodium (NaKα) and chloride (ClKβ) significantly increased when MPEO was loaded into porous chitosan nanostructure (Ahmed & Fekry, 2013; Beyki et al., 2014).

3.3. FTIR analysis of MPEO-CsNPs

Fig. 3. shows the FTIR spectra of chitosan and MPEO-CsNPs where some changes occur in the signals assigned to the formation of MPEO-CNs. Two distinctive signals are known as functional groups in chitosan molecule including a broad signal at 3415 cm^{-1} and a stretching signal at 2925 cm^{-1}, which are assigned to existing OH and NH. The signal at 1737 cm^{-1} on chitosan spectrum was attributed to the C═O in the carboxylic groups, which were probably overlapped by the incorporation of MPEO. A new signal which appeared at 2361cm^{-1} was attributed to electrostatic interactions of amine groups in chitosan with phosphoric units of TPP within the MPEO-Cs nanostructure (Haider, Majeed, Williams, Safdar, & Zhong, 2017; Ebrahimipour et al., 2014; Marzban, Ebrahimipour, & Danesh, 2016).

Fig. 4 represents size distribution and zeta potential of chitosan and chitosan-MPEO nanostructure. In Fig. 4a and b, z-average of chitosan and chitosan-MPEO was found to be 567.1 d.nm and 575.6 d.nm, respectively. Besides, the polydispersity index (PDI) for both chitosan and chitosan-MPEO was 0.325 and 0.584, respectively, in an increasing status as corresponding to z-average. Consequently, incorporation of MPEO into porous nano-polymeric chitosan caused a reduction in monodispersity of the nanoparticles and then increase in z-average indicating the expansion of the size dimension of nanoparticles. These results are in line with some reports in the literature that have certainly shown an increase in the size of nanoparticles when chitosan nanostructures are incorporated into essential oils. In the Fig. 4a, the zeta potential of chitosan shows an unknown fluctuation within the nanostructure while, after the formation of MPEO-CsNPs, zeta potential value tended toward a harmonic distribution of positive charge within the nanoparticles (Fig. 4b).

3.4. Kinetic release of MPEO from chitosan nanogel

The amount of MPEO released at different times was measured at 275 nm as maximum absorption wavelength obtained in the initial steps of the experiments. As seen in Fig. 5, nearly 50% of loaded MPEO in chitosan nanogel was released after 360 min incubation at the solvent with ambient temperature.

This occurrence could be attributed to loading capacity of nanogel, the porosity of chitosan nanostructure and electrostatic interactions between the essential oil and chitosan when it was treated with a strong solvent like ethanol. On the other hand, the literature has shown that release kinetics could be efficiently affected by the particle size of this formulation. However, some authors stated that the major cause of the release was associated with the swelling and degradation of the

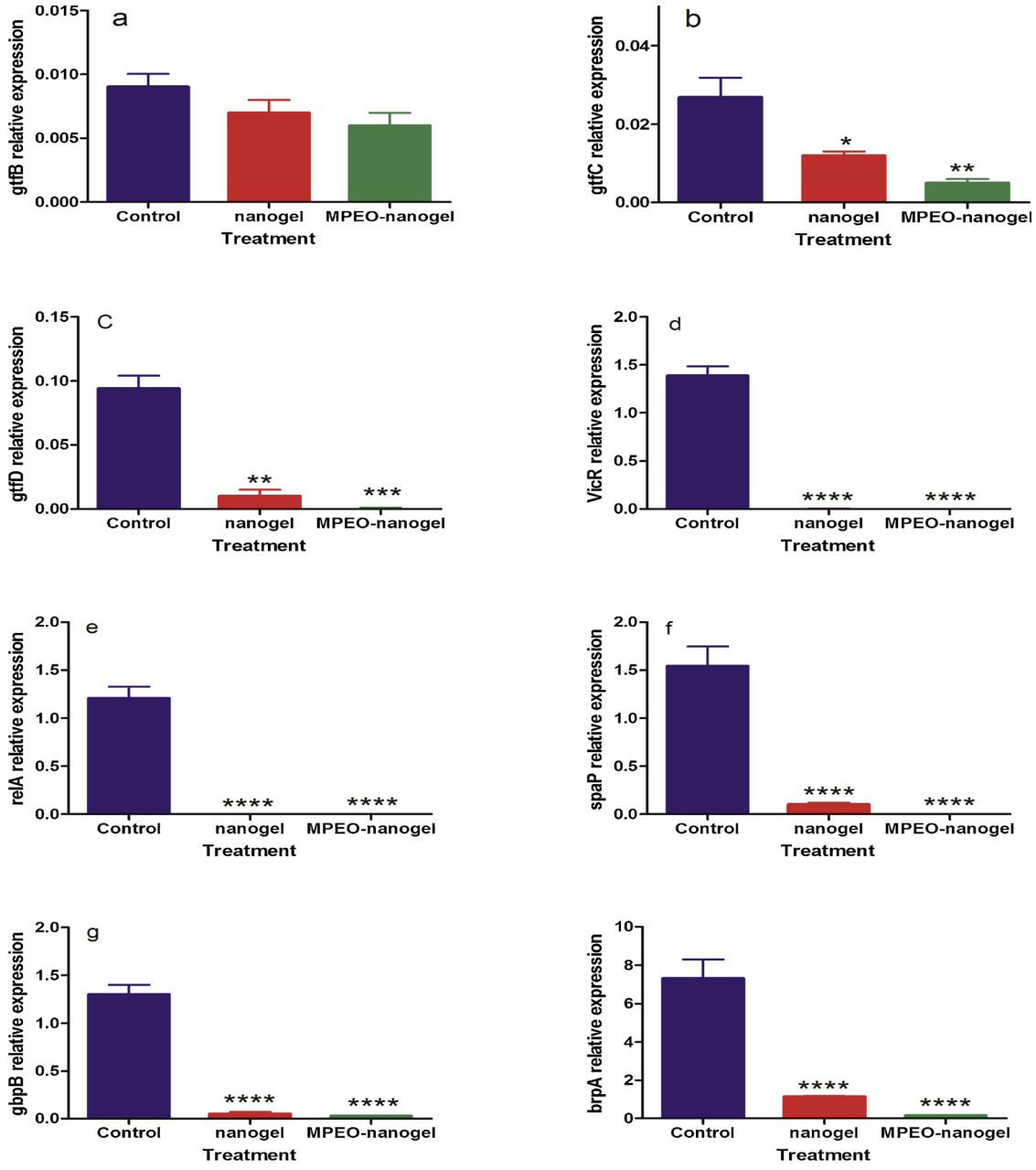

Fig. 7. Real-time PCR analysis of gene expression for 8 genes as virulence factor involved in biofilm formation. Significant levels were determined at $P < 0.05$ as one star (*), $P < 0.01$(**), $P < 0.005$ (***) and $P < 0.001$ (****) when compared with the control.

compacted chitosan–TPP nanoparticles. Hence, the results indicate that the chitosan–TPP nanosystem is suitable for controlling the release of MPEO. Taken together, considering the results of the release of MPEO, such releasing pattern could be desirable to inhibit biofilm formation, especially in dental health care.

3.5. Bacterial adherence

The adherence of the bacterial cells to dental surfaces was tested in the presence of different doses of MPEO-CNs. As seen in Fig. 6, the adherence of the bacterial cells was influenced in all the experiments that treated with MPEO-CNs from the dose of 7.5 to 250 µg/l. The results revealed that the adherence of bacterial cells had high sensitivity to the nanoformulation of MPEO, while when treated with unloaded CNs, had no inhibitory effect on adherence activity. *S. mutans* is a known biofilm producing bacterium, adhering to the dental surface in dental plaque in the mouth. Biofilms provide a non-penetrating barrier against the antibiotic therapy. Therefore, this form of bacterial colonization is considered as one-step of dental diseases, where MPEO-CNs could inhibit the synthesis of adhering factors by *S. mutans*.

3.6. Biofilm susceptibility assessment

MBIC value of MPEO-CsNPs and unloaded-nanogel against *S. mutans* was determined and presented in Table 3. Antibiofilm inhibition of *S. mutans* occurred at 50 µg/mL as the minimum dose of MPEO-CNs. This value for nanogel without essential oil was obtained at the highest dose tested, namely 400 µg/mL. The lowest dose of unloaded-nanogel was observed at about 35% biofilm inhibition, while MPEO-CNs in the same dose was able to inhibit 57% of biofilm formation. Therefore, MBIC for MPEO-CNs was approximately twofold compared to the control that was treated with no MPEO concentration.

3.7. Virulence gene expression analysis at presence of MPEO-CsNPs

As seen in Fig. 7, evaluation of biofilm gene expression including 8 genes responsible for biofilm formation was performed by real-time PCR technique. 16SrRNA gene was used as an internal control. Among these genes, *gtf*B, *gtf*C, *gtf*D that are glucosyltransferases (GTFase) enzymes were weakly affected by MPEO-CNs treatment, while *gbp*B, *spa*P, *brp*A, *rel*A, and *vic*R genes underwent significant down-regulation in the presence of both unloaded-nanogel and MPEO-loaded-nanogel. Expression of GTFase genes is considered as a promoting factor of biofilm synthesis because they produce glucan exopolysaccharides playing a critical role in bacterial adhesion and binding to dental surfaces. Besides, *gbp*B gene expresses an adhesion protein named glucan-binding protein B facilitating the binding of glucan to the physical and biological surfaces. The other genes such as *spa*P, *brp*A, *rel*A, and *vic*R encode the essential virulence factors that promote biofilm formation of *S. mutans in* different growth phases. One of the most important causes of dental caries is mouth-inhabiting bacteria. Hence, the dental structure was demineralized by bacterial by-products that originate from the metabolism of carbohydrate followed by acid production. On the other hand, bacterial colonization on the dental surface increases the disruptive effect that was initially driven by biofilm formation. Therefore, the reduction of biofilm formation by bacteria is considered as a logical approach to prevent bacterial plaque on the dental surface and to reduce acid production.

4. Conclusion

M. piperita essential oil was extracted and then a bioactive nanoformulation of MPEO loaded into chitosan was successfully prepared. The amount of initial MPEO affecting biofilm formation was in the range of nanogel loading capacity. SEM micrograph confirmed successful encapsulation of MPEO into porous chitosan nanostructure. The inhibitory effect of MPEO- CsNPs on the biofilm synthesis was revealed to be at the level of gene expression. MPEO-CsNPs showed a down-regulation effect on eight genes involved in biofilm and virulence factors causing bacterial adherence such as exopolysaccharides. Taken together, this study demonstrated that the MPEO- CsNPs promised an efficient nanoformulation with the greatest inhibitory action against some glycosyltransferase genes (*gtf*B, C and D) as important enzymes involved in extracellular polymers, subsequently inhibition of colonization of the bacterial cells at sub-MIC dose. Finally, the results concluded that MPEO-CsNPs could be potentially used as an antibiofilm agent in toothpaste or mouth washing formulations.

Acknowledgments

The research was supported through a financial grant [grant number A-10-1503-1] by Lorestan University of Medical Sciences and has been fulfilled in Razi Herbal Medicines Research Center.

References

Ahmed, R. A., & Fekry, A. (2013). Preparation and characterization of a nanoparticles modified chitosan sensor and its application for the determination of heavy metals from different aqueous media. *International Journal of Electrochemical Science, 8*(3), 6692–6708.

Anjum, R., & Malik, A. (2013). Evaluation of mutagenicity of wastewater in the vicinity of pesticide industry. *Environmental Toxicology and Pharmacology, 35*(2), 284–291.

Arshia Khan, A. K., Khan, K. M., Ahmed, A., Taha, M., & Perveen, S. (2017). Antibiofilm potential of synthetic 2-amino-5-chlorobenzophenone Schiff bases and its confirmation through fluorescence microscopy. *Microbial Pathogenesis, 110*, 497–506.

Barzegar, M., Ghaderi Ghahfarokhi, M., Sahari, M., & Azizi, M. (2016). Enhancement of thermal stability and antioxidant activity of thyme essential oil by encapsulation in chitosan nanoparticles. *Journal of Agricultural Science and Technology, 18*, 1781–1792.

Bernkop-Schnürch, A., & Dünnhaupt, S. (2012). Chitosan-based drug delivery systems. *European Journal of Pharmaceutics and Biopharmaceutics, 81*(3), 463–469.

Beyki, M., Zhaveh, S., Khalili, S. T., Rahmani-Cherati, T., Abollahi, A., Bayat, M., et al. (2014). Encapsulation of Mentha piperita essential oils in chitosan–cinnamic acid nanogel with enhanced antimicrobial activity against *Aspergillus flavus*. *Industrial Crops and Products, 54*, 310–319.

Cheung, R. C. F., Ng, T. B., Wong, J. H., & Chan, W. Y. (2015). Chitosan: An update on potential biomedical and pharmaceutical applications. *Marine Drugs, 13*(8), 5156–5186.

Ebrahimipour, G., Gilavand, F., Karkhane, M., Kavyanifard, A. A., Teymouri, M., & Marzban, A. (2014). Bioemulsification activity assessment of an indigenous strain of halotolerant *Planococcus* and partial characterization of produced biosurfactants. *International Journal of Environmental Science and Technology, 11*(5), 1379–1386.

Ebrahimipour, G., Moradi, A., Mehrdad, M., Marzban, A., & Alaee, H. (2011). Evaluation of antimicrobial substance produced by a bacterium isolated from *Parmacella iberica*. *Jundishapur Journal of Microbiology, 4*(3), 131–140.

El-Feky, G. S., Sharaf, S. S., El Shafei, A., & Hegazy, A. A. (2017). Using chitosan nanoparticles as drug carriers for the development of a silver sulfadiazine wound dressing. *Carbohydrate Polymers, 158*, 11–19.

Haider, J., Majeed, H., Williams, P. A., Safdar, W., & Zhong, F. (2017). Formation of chitosan nanoparticles to encapsulate krill oil (*Euphausia superba*) for application as a dietary supplement. *Food Hydrocolloids, 63*, 27–34.

Ikram, H., Rasool, N., Zubair, M., Khan, K., Abbas Chotana, G., Akhtar, M., et al. (2016). Efficient double suzuki cross-coupling reactions of 2,5-dibromo-3-hexylthiophene: Anti-tumor, haemolytic, anti-thrombolytic and biofilm inhibition studies. *Molecules, 21*(8), 977.

Keawchaoon, L., & Yoksan, R. (2011). Preparation, characterization and in vitro release study of carvacrol-loaded chitosan nanoparticles. *Colloids and Surfaces B: Biointerfaces, 84*(1), 163–171.

Kim, B.-S., Park, S.-J., Kim, M.-K., Kim, Y.-H., Lee, S.-B., Lee, K.-H., et al. (2015). Inhibitory effects of Chrysanthemum boreale essential oil on biofilm formation and virulence factor expression of *Streptococcus mutans*. *Evidence-Based Complementary and Alternative Medicine, 2015*.

Koo, H., Xiao, J., Klein, M., & Jeon, J. (2010). Exopolysaccharides produced by *Streptococcus mutans* glucosyltransferases modulate the establishment of microcolonies within multispecies biofilms. *Journal of Bacteriology, 192*(12), 3024–3032.

Kumari, A., Yadav, S. K., & Yadav, S. C. (2010). Biodegradable polymeric nanoparticles based drug delivery systems. *Colloids and Surfaces B: Biointerfaces, 75*(1), 1–18.

Marsh, P. D. (2010). Microbiology of dental plaque biofilms and their role in oral health and caries. *Dental Clinics, 54*(3), 441–454.

Marzban, A., Ebrahimipour, G., & Danesh, A. (2016). Bioactivity of a novel glycolipid produced by a halophilic Buttiauxella sp. and improving submerged fermentation using a response surface method. *Molecules, 21*(10).

Moghtader, M. (2013). In vitro antifungal effects of the essential oil of Mentha piperita L. and its comparison with synthetic menthol on*Aspergillus niger*. *African Journal of Plant Science, 7*(11), 521–527.

Mohammadi, A., Hashemi, M., & Hosseini, S. M. (2015). Chitosan nanoparticles loaded with *Cinnamomum zeylanicum* essential oil enhance the shelf life of cucumber during cold storage. *Postharvest Biology and Technology, 110*, 203–213.

Nagpal, K., Singh, S. K., & Mishra, D. N. (2010). Chitosan nanoparticles: A promising system in novel drug delivery. *Chemical & Pharmaceutical Bulletin, 58*(11), 1423–1430. https://doi.org/10.1248/cpb.58.1423.

Oh, J. K., Lee, D. I., & Park, J. M. (2009). Biopolymer-based microgels/nanogels for drug delivery applications. *Progress in Polymer Science, 34*(12), 1261–1282.

Oong, E. M., Griffin, S. O., Kohn, W. G., Gooch, B. F., & Caufield, P. W. (2008). The effect of dental sealants on bacteria levels in caries lesions: A review of the evidence. *The Journal of the American Dental Association, 139*(3), 271–278.

Rao, K. K., Reddy, P. R., Lee, Y.-I., & Kim, C. (2012). Synthesis and characterization of chitosan–PEG–Ag nanocomposites for antimicrobial application. *Carbohydrate Polymers, 87*(1), 920–925.

Saharkhiz, M. J., Motamedi, M., Zomorodian, K., Pakshir, K., Miri, R., & Hemyari, K. (2012). Chemical composition, antifungal and antibiofilm activities of the essential oil of *Mentha piperita* L. *ISRN Pharmaceutics, 2012*, 718645.

Sandasi, M., Leonard, C. M., Van Vuuren, S. F., & Viljoen, A. M. (2011). Peppermint (*Mentha piperita*) inhibits microbial biofilms in vitro. *South African Journal of Botany, 77*(1), 80–85.

Seneviratne, C. J., Zhang, C. F., & Samaranayake, L. P. (2011). Dental plaque biofilm in oral health and disease. *Chinese Journal of Dental Research, 14*(2), 87.

Singh, R., Shushni, M. A., & Belkheir, A. (2015). Antibacterial and antioxidant activities of *Mentha piperita* L. *Arabian Journal of Chemistry, 8*(3), 322–328.

Woranuch, S., & Yoksan, R. (2013). Eugenol-loaded chitosan nanoparticles: I. Thermal stability improvement of eugenol through encapsulation. *Carbohydrate Polymers, 96*(2), 578–585.

Wu, W., Shen, J., Banerjee, P., & Zhou, S. (2010). Chitosan-based responsive hybrid nanogels for integration of optical pH-sensing, tumor cell imaging and controlled drug delivery. *Biomaterials, 31*(32), 8371–8381.

Xiao, J., Zuo, Y., Liu, Y., Li, J., Hao, Y., & Zhou, X. (2007). Effects of Nidus Vespae extract and chemical fractions on glucosyltransferases, adherence and biofilm formation of *Streptococcus mutans*. *Archives of Oral Biology, 52*(9), 869–875.